

# MARIONET: An Exotendon-Driven Rotary Series Elastic Actuator for Exerting Joint Torque

James S. Sulzer, Michael A. Peshkin, and James L. Patton

**Abstract**— A cable-driven, rotary Series Elastic Actuator named MARIONET (Moment arm Adjustment for Remote Induction Of Net Effective Torque) is introduced as a novel means to deliver torque to a joint. Its advantages include remote actuation, independent control of compliance and equilibrium, and in future versions, the ability to span multiple joints. This cable-driven, compliant mechanism should prove very useful in a variety of human-robot interactions. Here we present a single joint device evaluated in terms of its position and torque step responses, its ability to follow a minimum jerk trajectory, and its ability to create torque fields. Results show that this device behaves as planned with several important limitations. We conclude with potential applications of this type of mechanism.

## I. INTRODUCTION

THERE are many different modalities for producing torque at a joint, and many unconventional methods can provide unique advantages to the field of human-robot interaction. Torque may be applied at the joint by motors, but doing this on a multilink system leads to carrying a heavy motor along with a segment which adds unwanted inertia into the system. Therefore, applying the torque from a remote location (the “base”) is desirable. Here, we propose a novel architecture, MARIONET, for delivering torque and demonstrate its utility through a simple device.

Some examples of robotic device that actuate at the base include BLEEX (Berkeley Lower Extremity Exoskeleton), which uses hydraulics to deliver power to the joints [1], and the MIT-MANUS, which exerts forces using a rigid linkage [2]. However, as the number of links and dimensions grow, such systems can become difficult to manage. Lightweight, remotely actuated cables can span multiple joints if they pass through the joint centers of proximal joints or if they are housed in sleeves (Bowden cables), like in a standard prosthetic arm, reducing this dimensional problem.

There exist a number of cable-driven human-robot

interactive devices. The UTAH-MIT hand [3], the String-Man [4], the WAM [5], the Phantom [6], and SpringWalker™ (Applied Motion, Inc.) are a few examples. Everyday devices such as bicycle and airplane brakes are classic uses of Bowden cables.

In each case mentioned above, the torque generated is a function of the tension in the cable. The cable is routed through a set of fixed points in space before reaching its target. Of interest in our design is the often-ignored portion of torque – the moment arm, or the cable’s line of action. Analogous to cables are biological muscles, and the importance of moment arms as well as the tension capabilities is now well understood [7-9]. Computational models can explore the kinetic relationship of how moment arms of muscles vary with joint angle [10].

We extend this concept by developing a device that directly controls torque by varying the moment arm. The MARIONET (Moment arm Adjustment for Remote Induction Of Net Effective Torque) uses cables and transmission to vary the moment arm. The result is a compliant, lightweight, compact, efficient and potentially inexpensive modality for torque production.

In the field of robotics, Series Elastic Actuators (SEAs) have drawn great interest. Composed of a motor in series with an elastic element, they are capable of accurate force control, energy storage, and filtering shock to the motor. In addition, smaller, less sophisticated motors may be used with a high friction, low backlash gear train [11]. Their inherent compliance is ideal for human-robot interaction [12], especially when dealing with neuromuscular difficulties such as spasticity.

The MARIONET is a type of SEA with variable stiffness and interesting applications. It introduces cable actuation to SEAs, leading to a more economic modality of torque production. Applications of this system include human-robot interactive situations such as a single joint manipulation, expansion to two or three joints, lower extremity training, and an exotendon system, where the cables are safely coupled to the user and the skeleton is used as rigid links.

We designed and built a single degree-of-freedom device to further explore its performance and its potential for expansion to multiple joints. The following analysis lays out the theoretical foundations on which more complicated mechanisms can be built. Below we define in detail the initial design, the rudimentary evaluation and the potential applications of this device.

Manuscript received February 16, 2005. This work was supported in part by the National Institute of Health T32 Training Grant, the Davee Foundation and the Faulk Trust.

James Sulzer is with the Laboratory for Intelligent Mechanical Systems and the Rehabilitation Institute of Chicago, USA 60611. (e-mail: sulzer@northwestern.edu).

Michael Peshkin is with the Laboratory for Intelligent Mechanical Systems at Northwestern University, USA 60208. (e-mail: peshkin@northwestern.edu).

Jim Patton is with the Rehabilitation Institute of Chicago, USA 60611. (e-mail: j-patton@northwestern.edu).

## II. CONCEPT OF THE MARIONET

### A. Rotational Variation of Moment Arm

The important question remains *how* to vary the moment arm in order to provide a stable and effective torque generation across all configurations. We considered three possibilities (Figure 1), where different paths of cable guidance compare with each other. The vertical guide path, a very large moment arm may be created, but it cannot exert torque on both sides of the center of rotation. The horizontal path is able to exert a torque on both sides of the center, but when the bar approaches a horizontal position, the mechanism is not capable of creating a torque. Avoiding both of these problems is a circular guide path, chosen because it has the ability to exert torque on both sides of the center as well as in any configuration (Figure 2). No torque is exerted when the position of the guide and bar coincide. This stable singularity is the source of global stability, another advantage of the configuration.

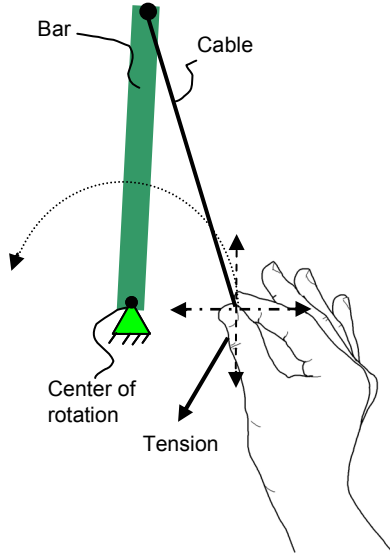


Fig. 1. Different paths of moment arm variation. Neither the vertical or horizontal guide paths were globally stable or capable of producing torque in every configuration. A circular path was chosen due to its inherent stability and its ability to exert torque on either side of the center of rotation.

### B. Schematic

Figure 2 details a more involved schematic of the circular guide path. The mechanism is composed of an actively controlled Rotator and a passive Link. The Rotator subsystem, has pulley guide is a distance  $r_P$  away from the center of rotation,  $x_C$ , with position  $\Phi$ . The position of the Rotator is controlled by the Drive motor at  $x_D$ . In (b), the Link (representing an arm) rotates around center  $x_C$ , with length  $r_L$  and position  $\Theta$ . A cable travels from a fixed point

## Rotator subsystem

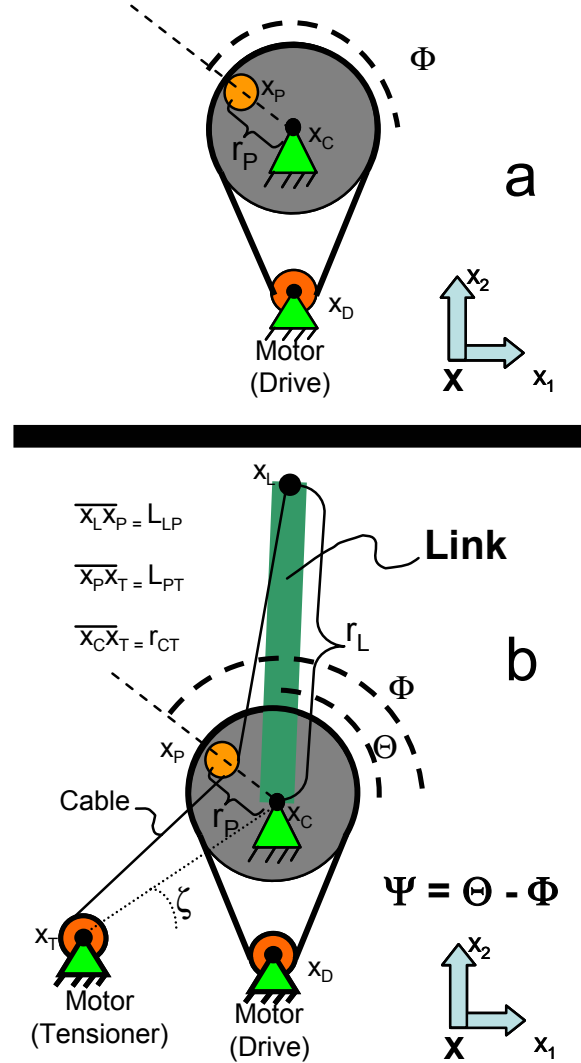


Fig. 2. Schematic of the MARIONET. The mechanism is composed of an active Rotator and a passive Link. In (a) above, the Rotator has a pulley to guide the cable (shown in b) a fixed distance ( $r_P$ ) away from center  $x_C$  at position  $\Phi$ . The Drive motor controls the position of the Rotator. Below, (b) shows the Link, with center  $x_C$ , position  $\Theta$  and length  $r_L$ . The Link and Rotator are coupled by a cable traveling from a tensioning motor through the Rotator pulley to the end of the link at  $x_L$ . The Link in this case is representative of a human arm.

on the Link,  $x_L$ , through the Rotator pulley at  $x_P$ , and then to a motor (Tensioner) at  $x_T$ . The Tensioner is located a fixed distance,  $r_{CT}$ , and angle  $\zeta$ , from the center. Note that the Rotator and Link have the same centers of rotation ( $x_C$ ) but each can rotate independently of the other. We imagine that later the link can be replaced by a human limb with only the cable present.

### C. Analysis

The system geometry of the MARIONET introduces an

inherent stiffness that allows an energy analysis for understanding its function. Assuming that the tension in the cable is constant, a conservative potential field is established and the energy is related to cable excursion (change in length of cable during operation) in the equation below,

$$\partial E = T \partial x, \quad (1)$$

where  $T$  is the tension and  $\partial x$  is the excursion of the cable. The excursion is an expression for the change in length of the cable. In this case, the total length of the cable is the sum of the length from the Link to the Rotator pulley ( $L_{LP}$ ) and the length from the Rotator pulley to the Tensioner ( $L_{PT}$ ),

$$x = L_{PT} + L_{LP}. \quad (2)$$

Using the Law of Cosines to solve for these lengths,

$$L_{PT} = \sqrt{r_p^2 + r_{CT}^2 - 2 \cos(\Phi - \zeta)} \quad (3)$$

$$\text{and } L_{LP} = \sqrt{r_L^2 + r_p^2 - 2 \cos(\Theta - \Phi)}. \quad (4)$$

The torque seen by the Link is a function of the relative angle between the Link and the Rotator and the tension. Since the energy is the integral of excursion, in rotational terms, the energy is

$$\partial E = \tau \partial \Psi, \quad (5)$$

where  $\Psi$  is the relative angle between the Link and the Rotator ( $\Theta - \Phi$ ), and  $\tau$  is the torque. Combining (1) and (5),

$$\tau = T \frac{\partial x}{\partial \Psi}. \quad (6)$$

Substituting (2) into (6), the resulting equation for torque is

$$\tau = T \frac{r_L r_p}{L_{LP}} \sin \Psi. \quad (7)$$

Note that torque is a function of tension and the relative angle  $\Psi$  only, and does not depend on the current position of the link – an advantage of a circular path. When  $\Psi$  is zero, the torque is also zero and is a position of minimal potential energy (a stable equilibrium) at the position of the Rotator.

The geometry creates the effect of a torsional spring that is linear for small values of  $\Psi$  and safely saturates at higher levels (see Figure 4). The result is a system that can continuously and independently set two control settings: equilibrium position (by positioning the Rotator) and stiffness (by adjusting tension,  $T$ ).

#### D. MARIONET as a Series Elastic Actuator

As stated in the introduction, the MARIONET belongs to the family of mechanisms known as Series Elastic Actuators (SEAs). Introduced by Pratt and Williamson [13], a number of robots, such as Cog [14], a single joint arm [15] and Spring Turkey [16], use SEAs for control. The MARIONET shares the same potential advantages of Series Elastic Actuators such as the ability to use a high gear ratio and a less sophisticated Drive motor, safer compliant operation, and independent control of both equilibrium position and stiffness. However, the current version of the MARIONET does not use an elastic element, apparently contradicting the definition of an SEA. Although no elastic element is used, the system moves against a conservative force field created by the Tensioner. Hence, the system does behave like an SEA. The MARIONET also differs from previous work by introducing cables for multiple joint actuations, possibly eliminating the need for robotic links. By safely coupling the cables to the user, the user's own skeleton provides the necessary rigidity, making it an excellent tool for rehabilitation robotics and other human-machine uses. As opposed to a strictly robotic device, the impedance of the user substitutes for a controlled impedance, making control less complicated.

#### E. Design of initial MARIONET device

The basics of the design are described in Figure 3. In the Link subsystem (a), the position of the Link,  $\Theta$ , is measured by a 10 k $\Omega$  potentiometer (JDK Controls) with a resolution of 0.03°. The Link pulleys, located at position  $x_L$ , are part of a block and tackle. The Rotator subsystem (b) is driven with a sprocket gear and roller chain (SDP-SI) by an AC servomotor (Yaskawa SGM-02B312), or Drive motor. The position of the Rotator,  $\Phi$ , is measured by the encoder on the servomotor, with a resolution of 0.016°. The Drive motor is operated in torque mode, using a PID to control position. The path of the cable is seen in (c), arranged in a block and tackle to amplify the effect of tension. The cable has one end anchored to the shaft of the Rotator pulleys, then wraps around the Link and Rotator pulleys twice. This results in a four-fold increase of effect of tension. The cable then passes through a number of fixed guide pulleys, and then to a spool, driven by the Tensioner motor (Yaskawa SGM-02B312). The Tensioner operates in an open loop torque mode, with a resolution of 0.16 N. A follower, similar to those used in fishing reels, is used here to guide the cable into the threads of the spool.

All motors and sensors are interfaced with a computer running QNX 6.2 RTOS. Data are sampled at 2 kHz.

### III. PERFORMANCE EVALUATION

The performance of the MARIONET was gauged by several experiments. First, we measured the torque generated by MARIONET and compared it to the predicted theoretical values. Next, we measured both position and torque step responses to characterize the system dynamics at different tension levels. We tested the position accuracy of the system by moving an artificial arm through a smooth trajectory, typical in rehabilitation applications. Finally, we analyzed the mechanism's ability to produce position- and velocity-dependent torque fields, another rehabilitation application.

#### A. Constant Tension Torque Accuracy

Since friction and unmodeled kinetics may lead to inaccuracies, the first test simply evaluated the theoretical torque relation (Equation 7). A passive tension was created using a 14.6 N weight hung over a pulley in place of the Tensioner, resulting in approximately 60 N of "effective tension" when the effect of the block and tackle is considered. All future tension values will be mentioned in terms of effective tension. With the Link held fixed, the Rotator position was varied causing changes in the reading of a load sensor attached to the end of the Link. Figure 4 demonstrates that the system does behave according to the theoretical sinusoidal relationship of (7).

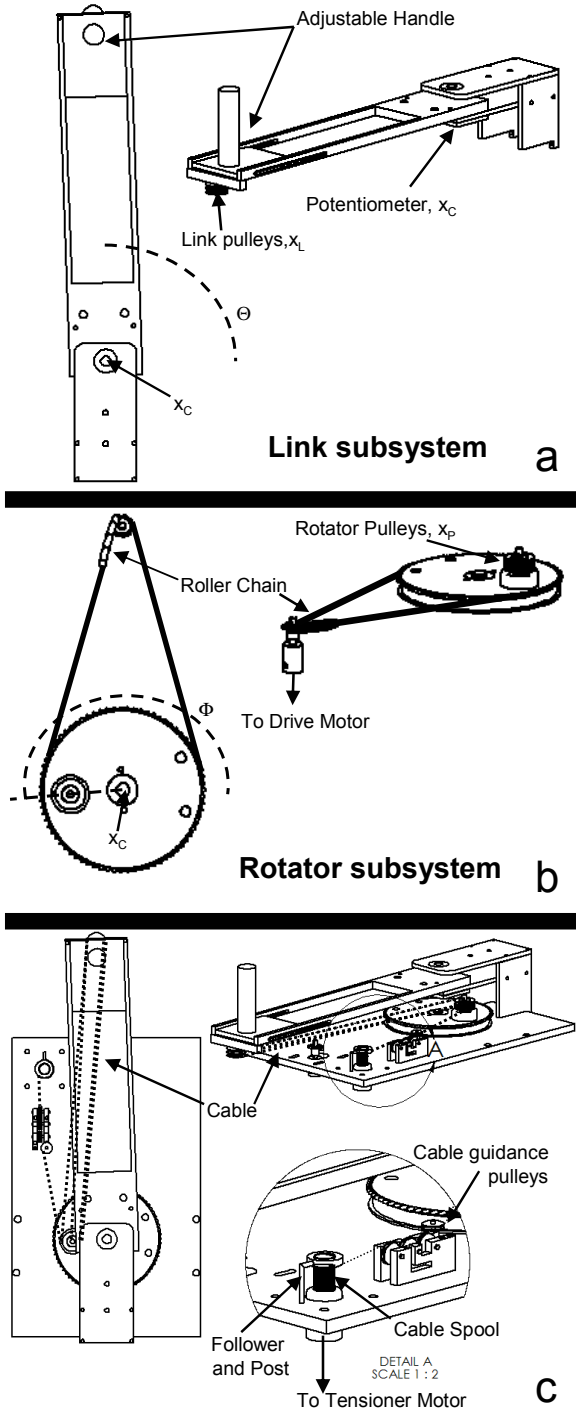


Fig. 3. Design of the MARIONET. (a) shows the Link subsystem, with a potentiometer for position,  $\theta$ . The adjustable handle can fit a variety of users. Link pulleys are located at the end of the Link to guide the cable shown in (c). The Rotator subsystem (b) is driven with a sprocket and chain (roller chain segment shown for visualization) by the Drive motor. The encoder on the motor gives the position of the Rotator. How the cable couples the two subsystems is shown in (c). A block and tackle wraps around the Rotator and Link pulleys (anchored to the shaft of the Rotator pulleys) to amplify the effect of tension. The cable passes through guidance pulleys until it reaches a cable spool. A follower keeps the cable in the threads of the spool, and the post keeps the follower from rotating with the spool. The Tensioner motor controls the tension in the cable.

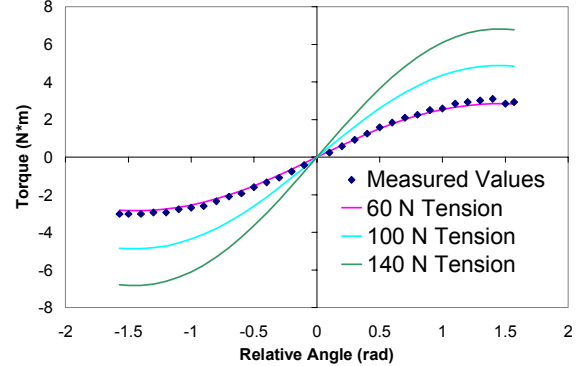


Fig. 4. Verifying theoretical accuracy. Using passive tension because of the large amount of friction produced by the follower, the MARIONET behaves according to theoretical predictions. Note the amplitude of torque increases with tension.

#### B. Position Step Response

Figure 5 displays the response of 0.3 rad position step input (step created by driving Rotator,  $\Phi$ ). To create a more realistic situation, we created an artificial arm with average mass and geometry characteristics of a human [17], sheathed it in foam insulation to simulate joint impedance, and then anchored to the arm on the device. The responses of the Link (with the artificial arm) to high tension (300 N) and low tension (70 N) are summarized in Table I. Overshoot, which was dampened by the friction of the artificial arm, was similar in the two trials, while the rise time and settling time both decreased as tension increased. Note that all tension values include the effect of the block and tackle.

### C. Torque Step Response

In this experiment, the Link was held fixed, and the relative angle  $\Psi$  was moved (by changing  $\Phi$ ) to a nominal 4.0 Nm torque at both high and low tension. Results can be seen in Table I. Lower tensions required a higher relative angle  $\Psi$  to achieve the same torque (7), thus longer to reach their maximum torque. Under higher tension (and smaller angle), there was a shorter rise time. However, the higher tension resulted in a saturation of the Drive motor, pulling the Rotator off position. This experiment identified the new design criteria that a MARIONET Rotator system must balance the need for speed that can alter torques at a sufficiently fast rate, and yet be strong and robust enough to assure that the Rotator moves to the commanded position. Optimally-gearred systems can accomplish this.

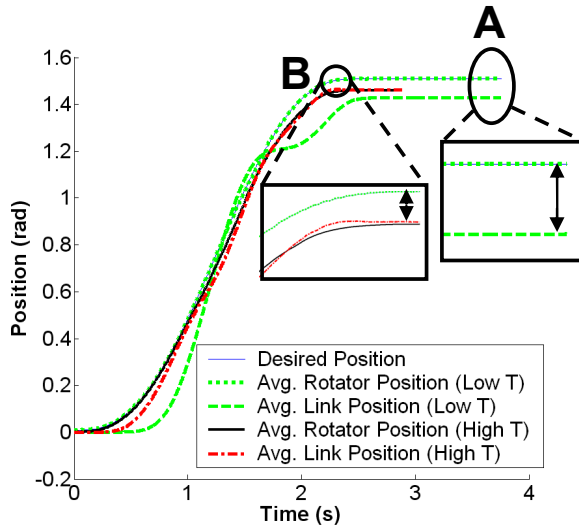


Fig.5. Analyzing Trajectory Error. Two types of errors occur in this response. At low tension, (A) shows that while the Rotator follows the desired position, the tension does not provide enough force to keep the Link on path. Note that the Rotator position (Low  $T$ ) and the desired position overlap. At high tension, (B) shows that the Link does have enough force to keep on the Rotator path, but the high tension causes the Drive motor to saturate, deviating slightly from the desired position.

### D. Minimum Jerk Trajectory Performance

A potential application of the MARIONET is rehabilitation, which would require that the system be able to guide a limb with compliance along a smooth trajectory. We chose a typical desired trajectory of 1.5 rad with duration of 2.5 seconds according to the minimum jerk pattern of movement [18]. Figure 5 demonstrates that at low tension, the deviation from the path is due to friction in the system and the impedance of the artificial arm. At high tension, again the Rotator position is slightly drawn away from the desired position because the Drive motor is not quite strong enough to resist the tension in the cable from the

source. Nevertheless, the system followed quite well (average error of only 0.04 rad, or 2.5°). A more robust Rotator system could have produced a more accurate path.

TABLE I  
COMPARISON OF MARIONET PROPERTIES

Experiment	Property	Low Tension	High Tension
Position Step Response	5% Rise Time	0.426 s	0.217 s
	5% Settling Time	1.77 s	1.12 s
	Overshoot	50.0%	55.6%
Torque Step Response	5% Rise Time	0.065 s	0.021 s
Min. Jerk Trajectory	Average Error	0.083 rad (4.76°)	0.044 rad (2.52°)

### E. Torque Field Performance

A short-term goal of the MARIONET involves training using torque fields. As stated previously in the mathematical analysis, the torque changes sinusoidally with the relative angle, yet with control software, the torque field does not have to be sinusoidal. Since the angle of the Rotator,  $\Phi$ , is controlled, the relative angle can be manipulated to create various shapes. In the following experiment, we examined both linear position- and velocity-dependent torque fields (Figure 6). While a linear path is the case with this experiment, various torque functions may be created by manipulating the relative angle.

With constant tension, a conservative, guiding (stabilizing) torque field can be created naturally with the MARIONET. However, a destabilizing (error-augmenting) torque field is also relevant to rehabilitation [19, 20, 21], and therefore both modalities are shown simultaneously. The torque field operates with a deadband in the middle, whose boundaries are chosen arbitrarily. For the position-dependent case in (a), the device creates a stabilizing modality quite well. However, in the destabilizing modality, the system faults at negative torques. This is due to Drive motor saturation, as seen in earlier experiments. The velocity-dependent case in (b) tells a different story. While again, the stabilizing modality is fairly accurate (with some error due to encoder filtering), the destabilizing modality faults at high velocities. This is in part due to encoder filtering as well, but mostly because of the quick directional change needed of the Rotator in a negative viscous torque field. Future designs will incorporate a more powerful drive motor and more sensitive position sensors.

## IV. SUMMARY AND CONCLUSIONS

The MARIONET is capable of delivering torque to a joint with advantages that include remote actuation, independent control of compliance and equilibrium, and the ability to span multiple joints. Despite some mechanical issues like friction and a relatively weak Drive motor, the device worked as planned and could follow a minimum jerk trajectory with a small amount of error. The system is suited

well for a position-dependent torque field, but in its current state is insufficient for a velocity-dependent field. Future development will involve resolving mechanical issues, experimentation with torque fields, expanding the mechanism to multiple joints, and even an extendon system, coupling the cables safely to the user. This cable-driven, compliant mechanism should prove very useful in a variety of human-robot interactions, including walking devices, limb exoskeletons, prosthetic limbs, and orthotic assist devices.

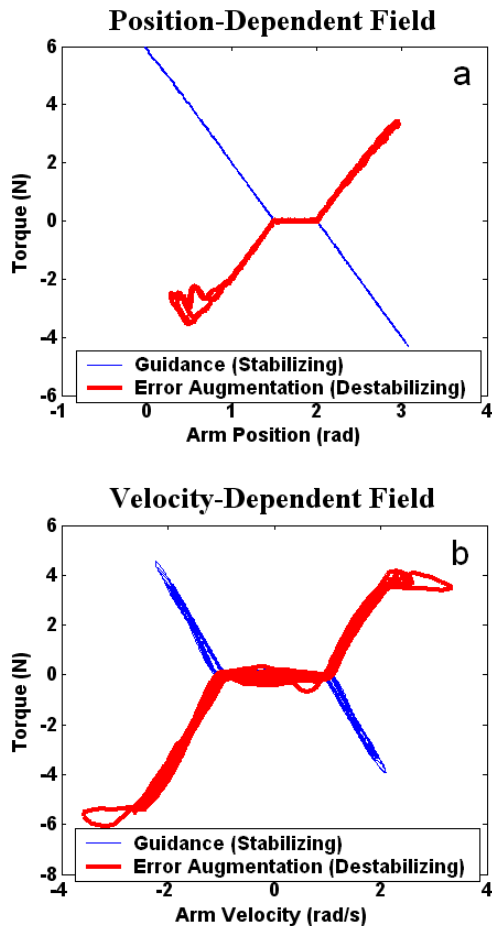


Fig. 6. Analyzing Torque Fields. Using a linear torque field, the position-dependent case in (a) is quite capable of creating a stabilizing or destabilizing field, except in the destabilizing negative torque case where the Drive motor is saturated. In (b), the performance of the stabilizing case is sufficient, but too much jerkiness occurs in the destabilizing case.

#### ACKNOWLEDGMENTS

We thank Richard Dojutrek and Robert Taglia for their support in building the device, and Eric Faulring for his help implementing the real-time control algorithm.

#### REFERENCES

[1] Tressler, J.M., T. Clement, H. Kazerooni, M. Lim. "Dynamic Behavior of Pneumatic Systems for Lower Extremity Extenders," presented at 2002 IEEE International Conference on Robotics and Automation, Washington D.C.

[2] Hogan, N., H.I. Krebs, J. Charnarong, P. Srikrishna, A. Sharon. "MIT-MANUS: A Workstation for Manual Therapy and Training. I," Proc. IEEE International Workshop on Robot and Human Communication, 1992.

[3] Jacobsen, S.C., E.K. Iversen, R.T. Johnson, D.F. Knutti, K.B. Biggers. "The Design of the Utah/MIT Hand," Proc. IEEE International Conference on Robotics and Automation, San Francisco, CA, 1996.

[4] Surdilovic, D., R. Bernhardt, T. Schmidt, and J. Zhang. "STRING-MAN: A New Wire Robotic System for Gait Rehabilitation," Proc. 8<sup>th</sup> International Conference on Rehabilitation Robotics, 2003.

[5] Salisbury, K., B. Eberman, M. Levin, and W. Townsend, "The Design and Control of an Experimental Whole-Arm Manipulator," Proc. 5<sup>th</sup> Int. Symp. On Robotics Research. 1989.

[6] SensAble Devices, Inc., "The PHANTOM," literature from SensAble Devices Inc. 225 Court St. Vanceburg, KY 41179.

[7] M. G. Hoy, F. E. Zajac, and M. E. Gordon, "Musculoskeletal Model of the Human Lower Extremity: The Effect of Muscle, Tendon, and Moment Arm on the Moment-Angle Relationship of Musculotendon Actuators at the Hip, Knee, and Ankle," in Journal of Biomechanics, vol. 23, 1990, pp. 157-169.

[8] M. L. Audu and D. T. Davy, "Influence of Muscle Model Complexity in Musculoskeletal Motion Modeling," in Journal of Biomechanical Engineering, vol. 107, 1985, pp. 147-157.

[9] R. M. Alexander and R. F. Ker, "The architecture of leg muscles," in Multiple Muscle Systems, J. M. W. a. S. L.-Y. Woo, Ed. New York: Springer-Verlag, 1990, pp. 568-577.

[10] S. L. Delp, J. P. Loan, M. G. Hoy, F. E., and F. E. Zajac, "Interactive Graphics-Based Model of the Lower Extremity to Study Orthopaedic Surgical Procedures," in IEEE Transactions on Biomedical Engineering, vol. 37, 1990, pp. 757-767.

[11] Pratt, G. A., M. M. Williamson, P. Dillworth, J. Pratt, K. Ulland, A. Wright. "Stiffness Isn't Everything," Proc. 4<sup>th</sup> International Symposium on Experimental Robotics, Stanford, CA, 1995.

[12] Raibert MH (1986) Legged robots that balance. MIT Press, Cambridge, Mass

[13] Pratt, G.A., and M. M. Williamson. "Series Elastic Actuators," Proc. IEEE/RSJ International Conference on Intelligent Robotics and Systems, Pittsburgh, PA, 1995.

[14] Brooks, R.A., and L.A. Stein. "Building Brains for Bodies," Autonomous Robots, 1994.

[15] Morita, T., and S. Sugano. "Development of One-D.O.F. Robot Arm equipped with Mechanical Impedance Adjuster," Proc. IEEE/RSJ International Conference on Intelligent Robotics and Systems, Pittsburgh, PA, 1995.

[16] Robinson, D.W., J.E. Pratt, D. J. Paluska, and G.A. Pratt. "Series Elastic Actuator Development for a Biomimetic Walking Robot," Proc. IEEE/ASME International Conference on Advanced Intelligent Mechatronics, Atlanta, GA, 1999.

[17] Winter, D. *Biomechanics and Motor Control of Human Movement*. New York, NY. John Wiley & Sons. 1990. pp. 56-57.

[18] Flash T, Hogan N (1985) The coordination of arm movements: An experimentally confirmed mathematical model. Journal of Neuroscience 5: 1688-1703.

[19] Patton, JL, ME Phillips-Stoykov, FA Mussa-Ivaldi. "Performance improves with force-fields that enhance error in chronic hemiparetic stroke survivors" conditionally accepted pending revisions, *Experimental Brain Research*.

[20] Brewer B, R Klatky, Y Matsuoka (2005) Perceptual Limits for a Robotic Rehabilitation Environment Using Visual Feedback Distortion. IEEE Transactions on Neural Systems & Rehabilitation Engineering, in press.

[21] Emken JL, DJ Reinkensmeyer (2005) Robot-Enhanced Motor Learning: Accelerating Internal Model Formation During Locomotion by Transient Dynamic Amplification. IEEE Transactions on Neural Systems & Rehabilitation Engineering, in press